Int J Civ Eng (2018) 16:263–272
https://doi.org/10.1007/s40999-016-0122-2

RESEARCH PAPER

Experimental study and modeling of fiber volume effects on frost resistance of fiber reinforced concrete

Mahmoud Nili[1] · Alireza Azarioon[1] · Amir Danesh[1] · Ali Deihimi[2]

Received: 17 May 2016 / Revised: 30 October 2016 / Accepted: 3 November 2016 / Published online: 16 November 2016

Abstract In the present study, the effectiveness of fiber inclusion on enhancing frost durability was experimentally examined. Polypropylene fiber of 0.2, 0.3, 0.4, and 0.5% and steel fiber of 0.2, 0.4, 0.6, 0.8, and 1.0% by volume fraction were used. Additionally, reference and air-entrained specimens (with 5% air content) were prepared to compare the results. The water/cement ratio for all concrete mixtures was 0.465. The compressive and tensile strengths, and longitudinal strains of frost-exposed specimens were measured. The results showed that both fibers improved the frost resistance of concrete, and 1% steel fiber inclusion caused the samples to be safe against freeze–thaw cycles as well as air entraining. Minimum fiber volumes of 0.4 and 0.5% were required for frost resistance in the steel and polypropylene fiber specimens, respectively. The results were also numerically examined using an artificial neural network (ANN). Data analysis showed that the ANN was capable of generalizing between input and output variables with reasonably fine predictions.

Keywords Freeze–thaw cycles · Steel fibers · Polypropylene fibers · Air-entrained concrete · Strength properties · Artificial neural network

Abbreviations

A	Air percent
C	Number of cycles
f_c	Predicted compressive strength
f_c^{nor}	Normalized compressive strength
f_t	Predicted tensile strength
f_t^{nor}	Normalized tensile strength
P	Volume fraction of PP fibers (%)
S	Volume fraction of and steel fibers (%)
x_{max}	Maximum amount of input data
x_{min}	Minimum amount of input data
x_{nor}	Normalized input data
ε	Longitudinal strain
ε^{nor}	Normalized longitudinal strain

1 Introduction

Frost durability is a key characteristic of concrete in severe environments. It is the duty of engineers to improve the durability and prolong the service life of concrete in cold regions. Powers stated that the hydraulic pressure theory accounts for frost damage in concrete [1]. In this regard, when water freezes, a tensile force is exerted and internal cracks are induced in the body of the concrete. During thawing, the water moves through the cracks and expands them; it remains present there to cause more damage when freezing occurs again. This theory was accepted by many researchers only in very saturated conditions; Even Powers replaced it with the theory of osmotic pressure [2]. Despite

✉ Mahmoud Nili
nili36@yahoo.co.uk; nili@basu.ac.ir

Alireza Azarioon
azarioon@gmail.com

Amir Danesh
amir.danesh85@gmail.com

Ali Deihimi
a.deihimi@basu.ac.ir

[1] Department of Civil Engineering, Bu-Ali Sina University, Hamedan, Iran

[2] Electrical Engineering Department, Bu-Ali Sina University, Hamedan, Iran

the fact that frost mechanisms in concrete may be fully understood by engineers, frost action is still the main reason for the deterioration of concrete structures.

It is generally accepted that air-entrained agents can relieve internal pressure generated by volume expansion. Therefore, the use of entrained air with a size of 50–200 μm and a spacing factor of less than 0.2 mm (0.008 in) protects concrete from inner destruction [3]. Air entraining also adversely affects strength properties of concrete; therefore, contractors in cold regions prefer to produce non air-entrained concrete. That's why some researchers tried to use various types of fibers as a replacement for air-entrained agents. Their main findings are summarized in Table 1. Moreover, testing and assessing the freeze–thaw resistance of concrete with and without an air-entrained agent is complicated and time consuming. For this reason, finding proper design, production, and evaluation techniques which guarantee the frost resistance of concrete is still a vital necessity.

In the present study, fibers were used as an alternative for AE agents, because the inclusion of fibers in concrete, mortar, and cement paste enhances many engineering properties, such as flexural strength, fracture toughness, thermal shock strength, and resistance under impact loadings [15–21].

Furthermore, a faster method based on the artificial neural network (ANN) was also used for the gathered investigated data. This technique has been recently used by researchers in various structural material characterization and modeling studies. The use of back-propagation neural network (BPNN) for modeling the behavior of conventional materials such as concrete in the state of plane stress under monotonic biaxial loading is described [22]. Some researchers demonstrate the applicability of NNs to composite material characterization. They use the BP algorithm to predict the thermal and mechanical properties of composite materials [23–25].

Subsequently, the present research may answer questions regarding which types of fibers, steel or polypropylene may increase the frost durability of concrete and whether the fibers can behave as an AE agent for releasing exerted stress. Moreover, the efficacy of the results was examined using the ANN technique.

Table 1 Main findings of researches about fiber application in frost resistance of concrete

Concrete type	Fiber type	Main result(s)	References
Normal concrete	PP	When the fraction is within 0.15–0.18%, their impermeabilities and frost resistances are best	[4]
		PP fiber can increase the bond strength of frost-damaged concrete and fine aggregate concrete remarkably	[5]
		PP fiber influences on the mass loss of concrete noticeably, which can improve the frost resistance of concrete	[6]
		Different kinds of PP fiber have different influences on freezing resistance. Some types of PP fibers can improve it while others may not	[7]
		By adding polypropylene fiber to concrete, the loss of dynamic modulus was improved, and the flexural strength was increased obviously, but the compressive strength had no significant variance	[8]
	Steel	The short metallic fibers apparently contribute to frost resistance of FRC due to their positive effect on the bond strength between fibers and matrix	[9]
		The best performance of SFRC can be got when the fiber quantity is 1.5%	[10]
		Adding an appropriate amount of steel fiber into concrete can reduce the porosity and improve the compactness of concrete	[11]
		The presence of steel fiber proves to shrink the porosity and improve evidently the frost resistance of concrete. It is also shown that the steel fiber content has a great influence on the frost-resisting property of SFRC. The best performance of SFRC can be achieved when the volume fraction of steel fiber is 1.5%	
		Steel fibers can improve the frost resistance and carbonation of concrete, compared with plain concrete. Steel fibers can also reduce cracking, and improve the cracking resistance of concrete materials	[12]
Self-compacting concrete	PP	Polypropylene fibers in concrete seemed to prohibit the movement of water in the air void system so that a sudden internal collapse occurred before 300 frost cycles	[13]
	Steel	Steel fiber self-compacting concrete in freeze–thaw cycle can play constrained role in the quality loss, dynamic elastic modulus and intensity, and can significantly improve the SCC frost resistance. Within a certain range, the more steel fiber, the stronger of frost resistance	[14]

2 Materials and methods

2.1 Mix proportions

The maximum size of the aggregate used in this study was limited to 19 mm. The physical properties of the aggregates are provided in Table 2. A water-cement ratio of 0.465 was used. Ordinary Portland cement (type I) was obtained from the Hekmatan factory in Hamedan, Iran. A high range water-reducing agent with the commercial name of Glenium 110 P was used to adjust the workability of the concrete, and an air-entrained agent of Micro-Air 100IR was used to adjust the air content of concrete. Both were obtained from the BASF Company. Polypropylene and hooked-end steel fibers were employed in this work. The geometry and the properties of the fibers are provided in Fig. 1 and Table 3, respectively.

Tests were performed on 11 different mix designs. Table 4 presents the composition and fresh concrete properties of the mixes. The reference and air-entrained specimens are labeled as A_0 and AE, respectively. The steel fiber concrete specimens with 0.2–1.0% fiber are shown as S_1 to S_5. Similarly, the polypropylene fiber concrete specimens with 0.2–0.5% by volume fractions are shown as P_1 to P_4, respectively. The results of the slump test revealed that, by properly selecting the super-plasticizer, it was possible to make a workable fiber-reinforced mixture.

Each type of freshly mixed concrete was cast into cubic (100 mm), cylindrical (100 × 200 mm), and prismatic (75 × 102 × 406 mm) shapes for compressive, splitting tensile, and strain measurement tests, respectively.

Table 2 Properties of aggregates

Physical properties	Sand	Fine gravel	Coarse gravel
Specific gravity (SSD)	2.61	2.68	2.69
Water absorption (%)	1.92	0.52	0.59
Fineness modulus	3.4	–	–
Volumetric percent (%)	51	8	41

2.2 Artificial neural network

Artificial neural networks (ANNs) as information-processing systems have certain performance characteristics in common with biological NNs which consist of a large number of simple processing elements called neurons or nodes. The ANN is characterized by the following three functions: (1) the pattern of connections between the neurons, (2) the method by which the weight of connections is determined which is called training or learning algorithm, and (3) the activation function. The feedforward NNs trained with the back-propagation (BP) learning algorithm are the most widely used NNs [26, 27]. Determining the best values of all the weights is called training the ANN [28, 29].

The Levenberg–Marquardt (LM) algorithm, a standard second-order nonlinear least-squares technique based on the back-propagation process, was used to train the ANN models [30, 31]. The hyperbolic tangent function was also used as the activation function to determine the relationship between input and output of a node and a network.

In the present work, because of the behavior of hyperbolic tangent function, data was normalized in the 0.2–0.8 interval. Data scaling is important as a preprocessing stage to ensure that all variables receive equal attention during training. The output variables have to be scaled to be commensurate with the limits of the transfer functions used in the output layer [32]. Scaling of the data was done individually using the following equation [33]:

$$x_{\text{nor}} = a\left(\frac{x_i - x_{\min}}{x_{\max} - x_{\min}}\right) + b \tag{1}$$

where x_{nor}, $x_{\min}$, and $x_{\max}$ are normalized, minimum, and maximum amount of data, respectively, and a and b are 0.2 and 0.8, respectively.

For any given ANN and set of connection weight values and training set, there exists an overall root mean squared (RMS) error of prediction. Training was finished when the network found the lowest RMSE or when the RMSE had not changed during a number of iterations.

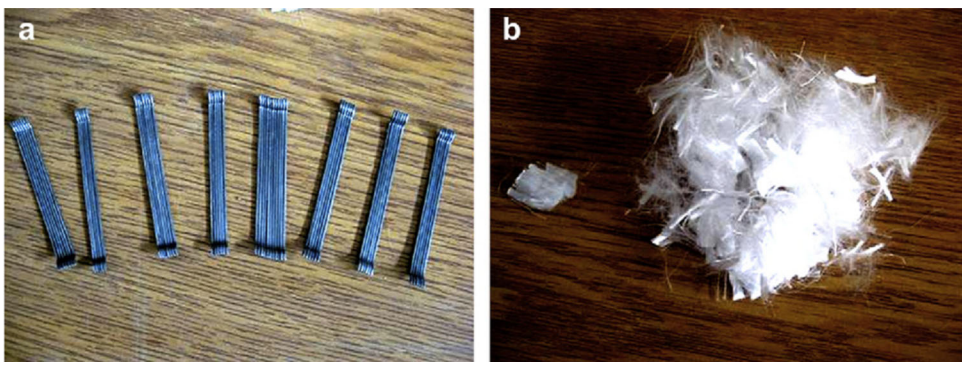

Fig. 1 Geometry and apparent shape of **a** steel, **b** polypropylene fibers

Table 3 Properties of fibers

Type of fiber	Length, l (mm)	Diameter, d (mm)	Aspect, ratio l/d	Density (g/cm^3)	Tensile strength (MPa)
Steel	60	0.75	80	7.8	1050
Polypropylene	12	0.022	545	0.91	350–400

Table 4 Mix proportions of the concrete mixtures

Mixture code	W/C	C (kg/m^3)	W (L/m^3)	Fine Agg. (kg/m^3)	Coarse Agg. (kg/m^3)	Steel fiber (%)	PP fiber (%)	A.E. (%)	S.P. (%)	Air content (%)	Slump (mm)
P_0S_0AE	0.465	385	179.05	881	847	–	–	0.07	–	5.0	70
$P_0S_0A_0$				918	881	–	–	–	0.55	1.8	80
$P_0S_1A_1$				915	879	0.2	–	–	0.6	–	80
$P_0S_2A_1$				912	877	0.4	–	–	0.75	–	80
$P_0S_3A_1$				909	874	0.6	–	–	0.9	–	80
$P_0S_4A_1$				907	871	0.8	–	–	1.0	–	75
$P_0S_5A_1$				904	869	1.0	–	–	1.2	–	70
$P_1S_0A_1$				915	879	–	0.2	–	0.95	–	80
$P_2S_0A_1$				914	878	–	0.3	–	1.3	–	70
$P_3S_0A_1$				812	876	–	0.4	–	1.4	–	65
$P_4S_0A_1$				811	875	–	0.5	–	1.5	–	60

Once the network is trained, the neural network may then be tested with unknown data, which has not been seen by the network [34, 35]. The ANN modeling was implemented within the MATLAB neural networks toolbox.

3 Testing procedures

Deterioration due to freeze-thaw cycles is assessed by various criteria, such as relative dynamic modulus of elasticity and length change (ASTM C666 [36]), mass loss (ASTM C672 [37]) and compressive strength (GOST 10060.0-95 [38], GOST 10060.1-95 [39]). In the present study, compressive and splitting tensile strength, and longitudinal strain as an index for length change are chosen.

Moreover, slow freeze–thaw cycles have been used by some researchers for better coincidence with real conditions [40–42]. In this research, a modified and more field representative testing procedure that involves slow freeze–thaw cycling is also used.

Compressive and tensile strength tests were carried out on the standard cured specimens at age 28 days. Furthermore, 60 slow freeze–thaw cycles were applied to 14-day cured specimens. The compressive strength, tensile strength, and longitudinal strain of the exposed specimens were measured every 20 freeze–thaw cycles. A system was designed to apply two freeze–thaw cycles (between −15 and +5 °C) every 24 h. The freezing and thawing periods were lengthened 8 and 4 h, respectively.

4 Experimental results

4.1 Compressive strength

The effects of the freeze–thaw cycles on compressive strength are summarized in Table 5. As shown, the compressive strength of the samples was decreased as the number of freeze–thaw cycles increased. This is due to the growth and propagation of cracks in the body of the concrete specimens [43–46].

As the compressive strengths are relatively close in various cycles, an error analysis is performed based on error propagation. Uncertainty of residual strength is calculated by multiplying the relative error and residual strength [47]:

$$\text{Uncertainty } (\%) = 100\left(\frac{f_c^0}{f_c^{60}}\right)\sqrt{\left(\frac{e_f}{f_c^{60}}\right)^2+\left(\frac{e_f}{f_c^0}\right)^2}, \qquad (2)$$

where f_c^0 and f_c^{60} are compressive strengths at 0 and 60 cycles, respectively. e_f is strength uncertainty, which equals to accuracy of device or 0.01 MPa. The maximum value of residual strength uncertainty is very slight and acceptable value of 0.045%.

The maximum decrease of 13.2% belonged to the reference specimens $P_0S_0A_0$. As shown, the increase in cycles had no negative impact on compressive strength of the air-entrained specimens. By addition of maximum amount of steel and PP fibers, the slight 1.54 and 3.42% decrease in compressive strength are achieved, respectively. The

Table 5 Compressive strength of concrete mixtures

Mix code	Compressive strength (MPa)					Residual strength (%)	Uncertainty (%)
	28 days	0 Cycle	20 Cycles	40 Cycles	60 Cycles		
P_0S_0AE	34.11	31.83	31.81	31.76	31.72	99.65	0.045
$P_0S_0A_0$	41.00	35.70	33.53	32.64	30.98	86.78	0.037
$P_0S_1A_1$	45.04	41.63	40.46	39.92	39.47	94.81	0.033
$P_0S_2A_1$	45.38	42.10	41.17	40.46	40.12	95.3	0.032
$P_0S_3A_1$	46.17	43.60	42.78	42.29	41.70	95.64	0.032
$P_0S_4A_1$	46.97	44.31	44.00	43.57	43.36	97.86	0.031
$P_0S_5A_1$	47.50	44.89	44.63	44.50	44.20	98.46	0.032
$P_1S_0A_1$	43.80	38.60	37.12	36.60	35.90	93.01	0.035
$P_2S_0A_1$	45.00	40.00	39.10	38.03	37.30	93.25	0.035
$P_3S_0A_1$	45.30	40.80	39.40	38.73	38.58	94.56	0.034
$P_4S_0A_1$	46.00	42.40	41.80	41.20	40.95	96.58	0.033

results also showed that the higher fiber volume fractions in the specimens led to a lower decrease of compressive strength.

Figures 2 and 3 illustrate the comparison of primary and residual compressive strength after 60 freeze–thaw cycles. The results show that the frost resistance of the steel fiber specimens (with 1% fiber) was similar to that for air-entrained (P_0S_0AE) specimens. Minimum fiber volumes of 0.4 and 0.5% lead to a residual strength more than 95% in the polypropylene and steel fiber specimens, respectively.

The fibrous concrete is higher in price than AE-concrete, however, the latter is not applicable easily in special concrete structures such as protective structures which should suffer both impact loading and freeze–thaw cycles simultaneously. This is the reason that the total cost of the fibrous concrete may be accepted by consumers.

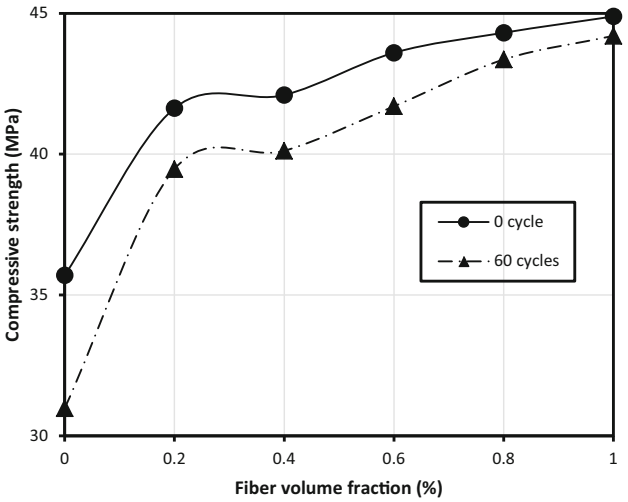

Fig. 2 Compressive strength of samples with steel fibers

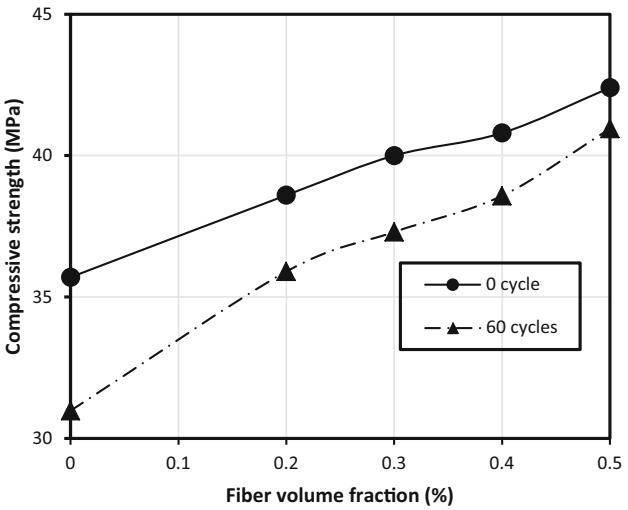

Fig. 3 Compressive strength of samples with PP fibers

4.2 Splitting tensile strength

The results of tensile strength tests for frost-attacked specimens are given in Table 6. An error analysis is done in a similar manner mentioned for compressive strength values. It can be seen that, by increasing the number of freeze–thaw cycles to 60, a considerable decrease of 37. 9% in tensile strength was observed in the referenced specimen; however, by addition of maximum amount of steel and PP fibers, the 5.35 and 21.74% decrease in compressive strength are achieved, respectively. This considerable difference suggests superiority of steel fibers to PP ones from tensile strength point of view. Increasing the fiber volume fraction led to less deterioration. Furthermore, the freeze–thaw cycles had no impact on the tensile strength of the AE or the high volume steel fiber specimens. These results are similar to those that were obtained for the compressive strength tests. Figures 4 and 5

Table 6 Splitting tensile strength of concrete mixtures

Mix code	Splitting tensile strength (MPa)					Residual strength (%)	Uncertainty (%)
	28 days	0 Cycle	20 Cycles	40 Cycles	60 Cycles		
P_0S_0AE	2.89	2.76	2.73	2.71	2.69	97.46	0.506
$P_0S_0A_0$	3.37	3.22	2.86	2.38	2.00	62.11	0.366
$P_0S_1A_1$	3.65	3.49	3.14	2.93	2.69	77.08	0.362
$P_0S_2A_1$	3.79	3.62	3.29	3.08	2.94	81.22	0.356
$P_0S_3A_1$	4.04	3.77	3.54	3.43	3.32	88.06	0.353
$P_0S_4A_1$	4.23	3.95	3.85	3.79	3.76	95.19	0.35
$P_0S_5A_1$	4.28	4.11	3.97	3.93	3.89	94.65	0.335
$P_1S_0A_1$	3.64	3.44	3.12	2.86	2.34	68.02	0.352
$P_2S_0A_1$	3.67	3.50	3.20	2.90	2.57	73.43	0.354
$P_3S_0A_1$	3.75	3.59	3.29	3.07	2.71	75.49	0.349
$P_4S_0A_1$	3.85	3.68	3.49	3.19	2.88	78.26	0.345

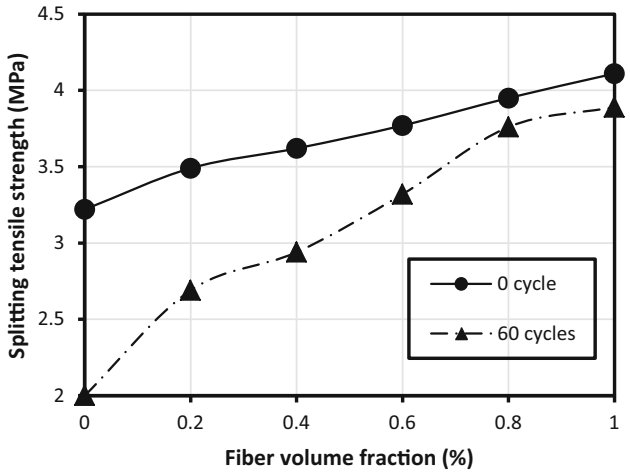

Fig. 4 Splitting tensile strength of samples with steel fibers

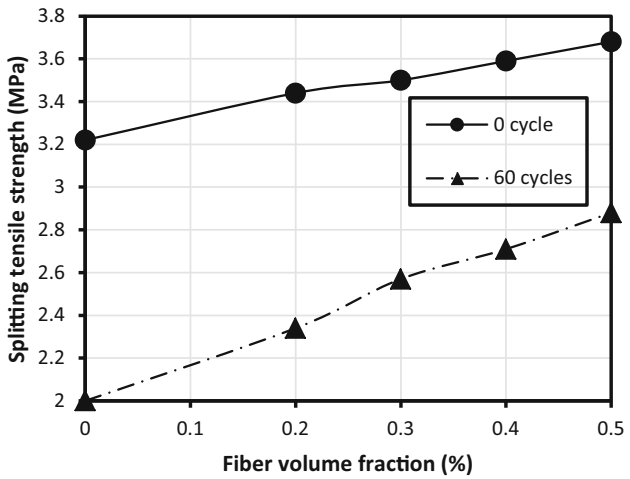

Fig. 5 Splitting tensile strength of samples with PP fibers

Table 7 Longitudinal strain of concrete mixtures

Mix code	Strain (%)		
	20 Cycles	40 Cycles	60 Cycles
P_0S_0AE	0.005	0.010	0.015
$P_0S_0A_0$	0.047	0.101	0.140
$P_0S_1A_1$	0.042	0.076	0.106
$P_0S_2A_1$	0.027	0.054	0.086
$P_0S_3A_1$	0.017	0.032	0.066
$P_0S_4A_1$	0.012	0.029	0.049
$P_0S_5A_1$	0.015	0.030	0.037
$P_1S_0A_1$	0.049	0.088	0.118
$P_2S_0A_1$	0.029	0.063	0.088
$P_3S_0A_1$	0.025	0.042	0.066
$P_4S_0A_1$	0.017	0.029	0.057

depict tensile strength and residual tensile strength after 60 freeze–thaw cycles

4.3 Longitudinal strain results

The measured longitudinal strains for the control, AE, and fiber-reinforced specimens are given in Table 7. It can be seen that the strains increased after freeze–thaw cycles; the maximum strain of 0.14% belonged to the reference specimen. A higher fiber volume fraction in the samples resulted in a lower increase in longitudinal strain. Figures 6 and 7 also show how strains of various mixes rose with freeze–thaw cycles. Similar to previous results of strength measurements, the positive effect of fiber volume fraction and the superiority of steel fiber compared with polypropylene fiber are obvious.

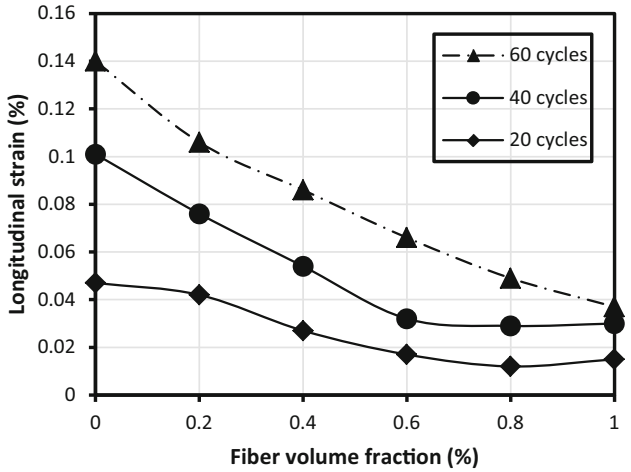

Fig. 6 Longitudinal strain of samples with steel fiber in various cycles

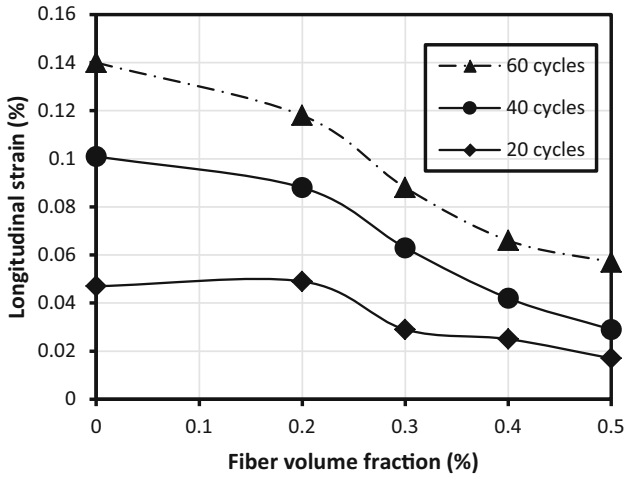

Fig. 7 Longitudinal strain of samples with PP fiber in various cycles

Figure 8 depicts the splitting tensile strength versus the longitudinal strain after 60 freeze–thaw cycles. It can be concluded that the decrease in strain agrees with the increase in longitudinal strain at high correlation coefficients of R^2 equaling 0.99 and 0.97 for steel and PP fiber, respectively.

5 Modeling results

In this study, the problem was proposed to the network models by means of four input and three output parameters. The parameters of air content, number of cycles, and percentage of steel and polypropylene fibers were selected as input variables. The output variables were compressive strength, tensile strength, and longitudinal strains.

The ANN model of compressive strength of samples is defined by the following expression:

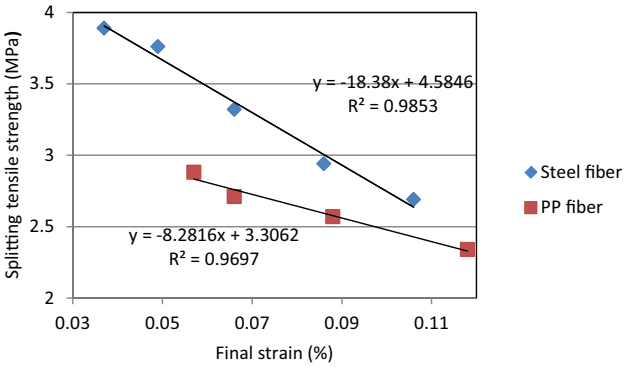

Fig. 8 Splitting tensile strength of fiber samples vs. final strain

$$f_c^{\text{nor}} = \begin{bmatrix} -1.8555 \\ -0.8882 \\ 0.9024 \end{bmatrix}^T \tanh \times \left(\begin{bmatrix} -0.3801 & -1.4636 & 2.2933 & 0.1461 \\ -0.6255 & -1.0427 & -0.0613 & 0.1904 \\ 0.1177 & 0.2845 & 0.1147 & 0.8956 \end{bmatrix} \begin{bmatrix} P \\ S \\ A \\ C \end{bmatrix} + \begin{bmatrix} 0.1102 \\ 0.2602 \\ -2.7691 \end{bmatrix} \right) + 0.50374, \tag{3}$$

where P, S, A, and C are volume fraction percentages of polypropylene and steel fibers, air percent, and number of cycles, respectively. Since the model gives normalized compressive strength (f_c^{nor}) in the [0.2, 0.8] interval corresponding the [31.72, 44.89] interval of ordinary compressive strength, the following linear relationship converts it into an ordinary compressive strength value (f_c), which was obtained based on linear interpolation:

$$f_c = 21.95 f_c^{nor} + 27.33 \tag{4}$$

Similarly, the ANN model of splitting tensile strength and longitudinal strain of samples are defined by the following expressions:

$$f_t^{nor} = \begin{bmatrix} -0.6365 \\ 1.3358 \\ 0.9043 \end{bmatrix}^T \tanh \times \left(\begin{bmatrix} 0.2084 & -2.4364 & 0.5829 & 0.1116 \\ -0.0085 & 1.4231 & 0.4952 & -0.1349 \\ 0.4832 & -0.5524 & -1.3084 & -0.4432 \end{bmatrix} \begin{bmatrix} P \\ S \\ A \\ C \end{bmatrix} + \begin{bmatrix} 1.8155 \\ 2.0848 \\ -1.5472 \end{bmatrix} \right) + 0.1063 \tag{5}$$

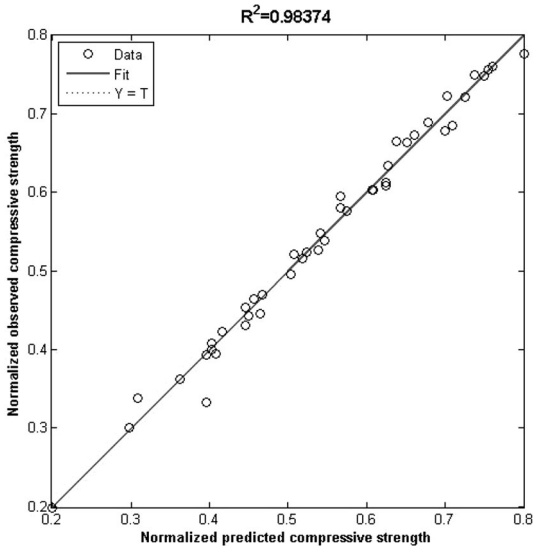

Fig. 9 Scatter plot of the observed versus predicted compressive strength of samples

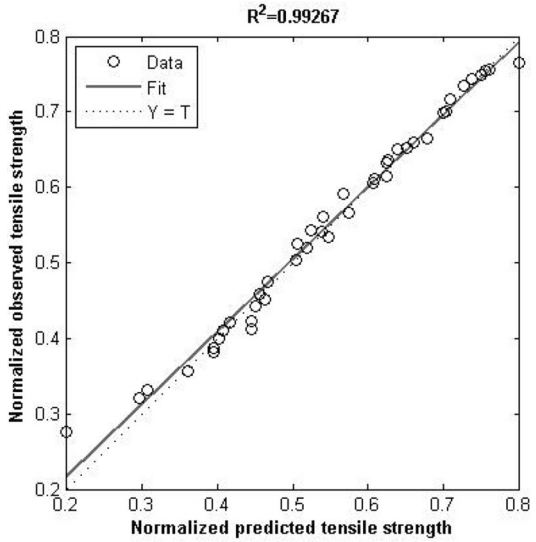

Fig. 10 Scatter plot of the observed versus predicted splitting tensile strength of samples

Linear interpolation corresponding to [0.2, 0.8] and [2, 4.11] intervals leads to:

$$f_t = 3.52 f_t^{nor} + 1.296 \tag{6}$$

$$\varepsilon^{nor} = \begin{bmatrix} -1.2084 \\ -1.4 \\ -1.2295 \end{bmatrix}^T \tanh \times \left(\begin{bmatrix} -1.7029 & -0.6266 & 1.1231 & 0.2233 \\ 0.8454 & 0.9907 & 0.0549 & -0.5268 \\ 0.0899 & 0.1871 & -0.5584 & -1.3015 \end{bmatrix} \begin{bmatrix} P \\ S \\ A \\ C \end{bmatrix} + \begin{bmatrix} -1.6411 \\ 1.7593 \\ -1.623 \end{bmatrix} \right) - 1.6018 \tag{7}$$

Similarly, Linear interpolation corresponding to [0.2, 0.8] and [0, 0.14] intervals leads to:

$$\varepsilon = 0.233 \varepsilon^{nor} - 0.0467, \tag{8}$$

where f_t and ε are splitting tensile strength and longitudinal strain, respectively. The performance of training and test sets are shown in Figs. 9, 10 and 11. It can be seen that the ANN model predicted the compressive strength, splitting tensile strength, and longitudinal strain with an R^2 of 0.98, 0.99, and 0.99, respectively.

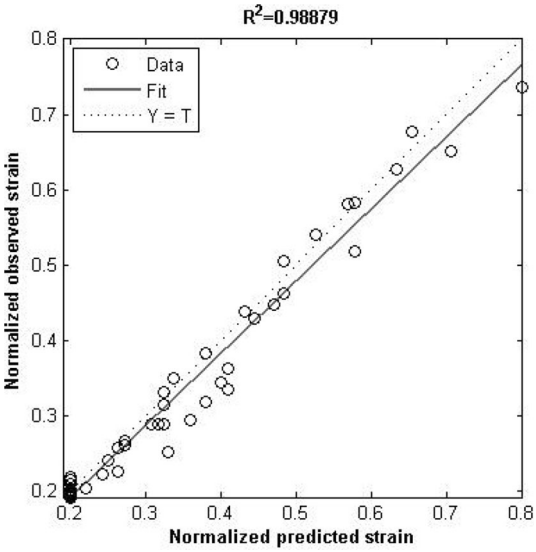

Fig. 11 Scatter plot of the observed versus predicted longitudinal strain of samples

6 Conclusions

1. The effect of fiber volume on the frost resistance of polypropylene and steel fiber specimens exposed to 60 slow freeze–thaw cycles was examined. The results were compared with the air-entrained specimen. The following conclusions can be drawn from the results.
2. Inclusion of fibers into the concrete specimens enhanced both the compressive and splitting strength of the specimens compared to those without fibers. The maximum strength of 47.5 MPa belonged to the 1% steel fiber specimens.
3. After 60 freeze–thaw cycles, the compressive strength of the specimens decreased 1.54 and 3.42% by addition of maximum amount of steel and PP fibers, respectively. The tensile strength of the specimens also decreased 5.35 and 21.74% by addition of maximum amount of steel and PP fibers, respectively, but the

strain of the specimens increased. As expected, the air-entrained sample attained the best resistance against freeze–thaw cycles.

4. Introducing fibers at a high fraction volume, in particular steel fibers, into the concrete mixtures prevented frost deterioration in the specimens. Minimum fiber volumes of 0.4 and 0.5% were required for frost resistance in the polypropylene and steel fiber specimens, respectively.
5. The frost resistance of the steel fiber specimen (1% fiber volume) was similar to that of the air-entrained ones.
6. From tensile strength point of view, Steel fiber is far more superior to PP, but steel fiber is only slightly better in compressive strength and strain changes of specimens.
7. The best correlation was obtained between decrease in splitting tensile strength and increase in strain of frost-exposed samples; this revealed that strain increase may be considered as a proper index for frost actions.
8. The ANN was found to be capable of generalizing between the input variables and the output of compressive and tensile strength and strain with good reasonable predictions.
9. From the viewpoints of strength and durability, steel fibers can improve frost durability without sacrificing strength. These important results can relieve engineers' anxiety about using air-entrained agents in concrete. Furthermore, AE-concrete is not applicable easily in special concrete structures such as protective structures, which should suffer both impact loading and freeze–thaw cycles simultaneously. This is the reason that the total cost of the fibrous concrete may be accepted by consumers.

References

1. Powers TC (1945) A working hypothesis for further studies of frost resistance of concrete. J ACI 16(4):245–272
2. Penttala V (2006) Surface and internal deterioration of concrete due to saline and non-saline freeze–thaw loads. Cem Con Res 36(5):921–928
3. Mehta PK, Monteiro PJM (2013) Concrete: microstructure, properties, and materials, 4th Ed., McGraw-Hill Professional
4. Cen GP, Ma GQ, Wang ST, Zhang LJ (2008) Durability of synthetic fiber reinforced concrete for airport pavement. J Traffic Transp Eng 8(3):43–51
5. Zhao J, Gao DY, Li GH (2009) Research on frost-damaged concrete strengthened with polypropylene fiber reinforced fine aggregate concrete. J Build Mater 12(5):575–579
6. Huo J, Yang H, Shen X, Cui Q (2011) Orthogonal experimental study on frost resistance of polypropylene fiber concrete. Adv Mat Res 152–153:1574–1578
7. Shi ZW, Liu S, Zhang RR (2011) Comparative experiment on frost resistance of different kinds of polymer fibrous concrete. Adv Mat Res 250–253:673–677
8. Chen, SP, Ten F (2015) Freeze-Thaw damage model for polypropylene fiber concrete, 4th International Conference on Civil, Architectural and Hydraulic Engineering, ICCAHE, Guangzhou, China, 121–126
9. Xu P, Yi C, Fan CM, Joshi RC(1998) Performance of fiber reinforced concrete with respect to frost resistance: A case study. Proceedings of the 9th International Conference on Cold Regions Engineering; Duluth, USA, 479–488
10. Jiang, L, Niu D, Bai M (2010) Experiment study on the frost resistance of steel fiber reinforced concrete. International Conference on Advances in Materials and Manufacturing Processes, ICAMMP. 243–246
11. Niu D, Jiang L, Bai M (2012) Experimental analysis on the frost resistance of steel fiber reinforced concrete. J Civil Archit Environ Eng 34(4):80–98
12. Zhang S, Dong X (2012) Effect of steel fiber on the performance of concrete materials. Appl Mech Mater 193–194:337–340
13. Persson B (2006) On the internal frost resistance of self-compacting concrete, with and without polypropylene fibers. Mater Struct 39(291):707–716
14. Gao M, Zhao Y, He X (2012) Research of steel fiber self-compacting concrete frost resistance. Appl Mech Mater 174–177:721–725
15. Dutta P (1988) Structural fiber composite materials for cold regions. J Cold Reg Eng 2(3):124–134
16. Khaloo A, Molaee A (2003) Freeze and thaw and abrasion resistance of steel fiber reinforced concrete (SFRC). IJCE 1(2):72–81
17. Nili M, Ghorbankhani AH, Alavi Nia A, Zolfaghari M (2016) Assessing the impact strength of steel fibre-reinforced concrete under quasi-static and high velocity dynamic impacts. Constr Build Mater 107:264–271. doi:10.1016/j.conbuildmat.2015.12.161
18. Lampropoulos AP, Paschalis SA, Tsioulou OT, Dritsos SE (2016) Strengthening of reinforced concrete beams using ultra high performance fibre reinforced concrete (UHPFRC). Struct, Eng. doi:10.1016/j.engstruct.2015.10.042
19. Perumal R, Nagamani K (2014) Impact characteristics of high-performance steel fiber reinforced concrete under repeated dynamic loading. IJCE 12(4):513–520
20. Ramadoss P (2014) Combined effect of silica fume and steel fiber on the splitting tensile strength of high-strength concrete. IJCE 12(1):96–103
21. Kamal M, Safan M, Etman Z, Abd-elbaki M (2015) Effect of steel fibers on the properties of recycled self-compacting concrete in fresh and hardened state. IJCE. 13(4):400–410
22. Ghaboussi J, Garrett JH, Wu X (1991) Knowledge-based modeling of material behavior with neural networks. J Eng Mech ASCE 117(1):132–53
23. Doh J, Lee SU, Lee J (2016) Back-propagation neural network-based approximate analysis of true stress-strain behaviors of high-strength metallic material. J Mech Sci Tech 30(3):1233–1241. doi:10.1007/s12206-016-0227-1
24. Karakoç MB, Demirboa R, Türkmen I, Can I (2011) Modeling with ANN and effect of pumice aggregate and air entrainment on the freeze-thaw durabilities of HSC. Constr Build Mater 25(11):4241–4249
25. Shi X, Akin M (2012) Holistic approach to decision making in the formulation and selection of anti-icing products. J Cold Reg Eng 26(3):101–117
26. Freeman JA, Sikapura DM (1991) Neural networks. Algorithms, applications, and programming techniques. Addison-Wesley Inc, USA
27. Anderson JA (1995) An introduction to neural networks. A Bradford book. MIT Press, Cambridge

28. Maren A, Harston C and Pap R (1990) Handbook of neural computing applications. Academic Press. Inc, USA
29. Dhar V, Stein R (1997) Intelligent decision support methods. Prentice-Hall Inc, USA
30. Hagan MT, Menhaj MB (1994) Training feed forward networks with the Marquardt algorithm. IEEE Trans Neural Network 5(6):861–867
31. Masters T (1995) Neural, novel and hybrid algorithms for time series prediction. Wiley, New York
32. Baziar MH, Saeedi Azizkandi A (2013) Evaluation of lateral spreading utilizing artificial neural network and genetic programming. IJCE 11(2):100–111
33. Altun F, Kisi O, Aydin K (2008) Predicting the compressive strength of steel added lightweight concrete using neural network. Comp Mater Sci 42(2):259–265
34. Parthiban T, Ravi R, Parthiban GT, Srinivasan S, Ramakrishnan KR, Raghavan M (2005) Neural network analysis for corrosion of steel in concrete. Cor Sci 47(7):1625–1642
35. Kim J, Kim D, Feng M, Yazdani F (2004) Application of neural networks for estimation of concrete strength. J Mater Civ Eng 16(3):257–264
36. ASTM C 666 (2008) Standard test method for resistance of concrete to rapid freezing and thawing
37. ASTM C 672 (2012) Standard test method for scaling resistance of concrete surfaces exposed to deicing chemicals
38. GOST 10060.0-95 (1995) Concretes. Methods for the determination of frost-resistance. General requirements, Russian National Standards
39. GOST 10060.1-95 (1995) Concretes. Basic method for the determination of frost-resistance, Russian National Standards
40. Pigeon M, Lachance M (1981) Critical air void spacing factors for concretes submitted to slow freeze-thaw cycles. ACI J 78(4):282–291
41. Amini B, Tehrani S (2011) Combined effects of saltwater and water flow on deterioration of concrete under freeze-thaw cycles. J Cold Reg Eng 25(4):145–161
42. Yang Z (2011) Freezing-and-thawing durability of pervious concrete under simulated field conditions. ACI Mater J 108(2):187–195
43. Marzouk H, Jiang D (1994) Effects of freezing and thawing on tension properties of HSC. ACI Mater J 91(6):577–586
44. Sabir BB (1997) Mechanical properties and frost resistance of silica fume concrete. Cem. Con. Compos. 19(4):285–294
45. Hori M, Morihiro H (1998) Micromechanical analysis on deterioration due to freezing and thawing in porous brittle materials. Int J Eng Sci 36(4):511–522
46. Cao DF, Ge WJ, Wang BY, Tu YM (2014) Study on the flexural behaviors of RC beams after freeze-thaw cycles. IJCE 13(1):92–101
47. Balagurusamy E (1999) Numerical methods. Tata McGraw Hill Publications Company, New Delhi